Analysis of two-phase ceramic composites using micromechanical models

P. Alveen[a], D. McNamara[a], D. Carolan[a,b], N. Murphy[a], A. Ivanković[a,*]

[a] *School of Mechanical and Materials Engineering, University College Dublin, Ireland*
[b] *Department of Mechanical Engineering, Imperial College London, London SW7 2AZ, UK*

Abstract

Micromechanical models of two-phase ceramic composites are created using a modified Voronoi tessellation approach. These representative Finite Volume (FV) microstructures are used to investigate the role of microstructure on fracture of advanced ceramics. An arbitrary crack propagation model using a cell-centred finite volume based method is implemented. In particular the effect of matrix content is examined. It is shown that the underlying microstructure significantly affects the local stress and strain distributions for a two-phase ceramic containing hard particles in a softer matrix. Simulation results indicate that an increase in the volume fraction of these hard grains leads to an increase in strength of the composite material. Furthermore, it is found that the homogeneity of the microstructure affects the overall strength.

Keywords: Microstructure, Voronoi tessellation, numerical model, finite volume analysis, brittle fracture

*Corresponding author
Email address: Alojz.Ivankovic@ucd.ie (A. Ivanković)

1. Introduction

Advanced ceramics are a class of materials which exhibit superior properties when compared to traditional ceramics, such as abrasion resistance and high hardness. Due to these superior properties, the materials often find use in extreme conditions involving high temperature and impact loading, for example as tool materials for high speed machining and rock drilling [1]. These extreme conditions may lead to premature failure due to fracture or chipping.

According to Groeber et al. [2] and Ayyar and Chawla [3] early methods for modelling of microstructures did not consider the actual particle shapes and instead used cubes, spheres and ellipsoids as an approximation of the particle shape. However, in reality microstructures are complex and it is well established that mechanical and fracture properties of ceramic materials are affected by the underlying microstructure [4–6]. It has been shown by Carolan et al. [7, 8] that the strength and toughness of certain advanced ceramics are affected by both the size of the primary phase and the percentage matrix content. Therefore it is desirable to be able to accurately model these microstructures in order to understand the mechanisms which contribute to failure and guide the development of improved materials. Furthermore, it is important to be able to correctly predict the stresses, crack initiation and propagation characteristics of complex microstructures [9].

Numerical models have been used extensively to model crack growth and in most cases this has been carried out using the Finite Element (FE) method [3]. However in the current work the Finite Volume (FV) method was implemented. Over the last number of years the FV method has become es-

tablished as an alternative to the FE method for the solution of problems involving stress analysis. The method was first developed for the solution of solid mechanics problems by Demirdžić and co-workers [10–14]. Ivanković and co-workers have applied the FV method successfully to the solution of both fracture problems [15–19] and fluid structure interaction problems [20, 21].

Numerous studies have been carried out to produce numerical microstructures using Voronoi tessellation [22, 24, 41]. It is well established that polycrystalline microstructures can be modelled using Voronoi tessellations. Nygårds and Gudmundson [25] use Voronoi tessellations to create 3D geometrical models of 2-phase ferrite/pearlite steel with periodic boundary conditions. Kühn and Steinhauser [26] model polycrystalline materials using power diagrams which are a generalisation of Voronoi diagrams for arbitrary dimensions. Voronoi tessellations have also been used to investigate fracture. Espinosa and Zavattieri [27] investigate failure initiation in brittle materials, while Warner and Molinari [28] model compressive fracture of alumina ceramics. Similar to the current study, Zhou et al. [29] and Wang et al. [30] have used Voronoi tessellations to investigate crack propagation in ceramic tool materials. Voronoi tessellations have also been used to investigate plasticity by modelling elasto-viscoplastic deformation of rubber-toughened glassy polymers [31].

Zhang et al. [33, 47] used a controlled Poisson Voronoi tessellation model to generate polycrystalline microstructures. They introduced control parameters to control the regularity of the microstructure and ensure that the grain size distribution is statistically equivalent to real microstructures. As men-

tioned previously this is important in the case of fracture problems where the microstructure morphology will affect fracture initiation.

Nygårds and Gudmundson [25], Li et al. [34] and Wang et al. [35] have all created 2-phase microstructures using Voronoi tessellations. In this study we examine a two-phase ceramic structure consisting of randomly dispersed hard particles held together with a softer matrix material. The matrix materials can be either ceramic or metallic.

2. Microstructure Generation

2.1. Voronoi tessellation approach

Voronoi tessellation was used to generate the geometrical model of the microstructure. It is a commonly used method for the generation of numerical microstructures of ceramic and metallic materials in both two- and three-dimensions. The Voronoi tessellation algorithm produces a random structure which is representative of a polycrystalline material as outlined in [36]. To create the two-phase ceramic structure each Voronoi tile is contracted around the circumcentre of the tile until the desired area fraction of the second phase is reached. When viewing micrographs of some advanced ceramics it may be observed that the grains cluster together resulting in regions filled predominantly with the second phase material. These regions will be referred to as matrix agglomerations (MA). In order to create these numerically a specified number of particles are removed from the synthetic microstructure while keeping the overall particle phase content constant, see Figure 1.

The generated microstructures were all 100×100 μm in size with an average particle area of 30 μm^2. The particle size distributions follow a lognormal

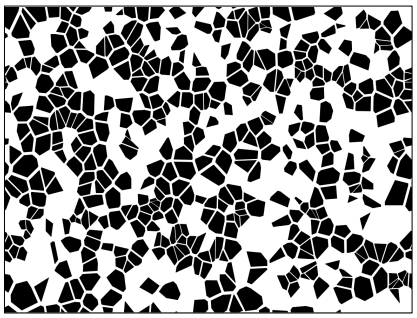

Figure 1: Numerical ceramic microstructure with 50% particulates and matrix agglomeration

distribution as outlined in [36]. The percentage particles was varied from 30% to 70% in increments of 10% as shown in Figure 2. Three different microstructures were generated for each volume fraction as it is expected that the geometrical variability on the microstructural level will affect the overall material. A further three 50% microstructures with matrix agglomerations were generated to investigate their effect on strength and fracture, see Figure 2f.

3. Analysis

3.1. Finite volume analysis

Finite Volume (FV) analysis was carried out on the numerical microstructures using OpenFOAM 1.6-ext [38–40]. The simulations were 2-dimensional and plane strain was specified in the third direction. The plane strain representation has been considered as an alternative to the more computationally demanding full three dimensional analysis. This approach has already been successfully adopted by several previous authors [30, 34, 41]. Both the particulates and matrix were treated as isotropic linear elastic over the course

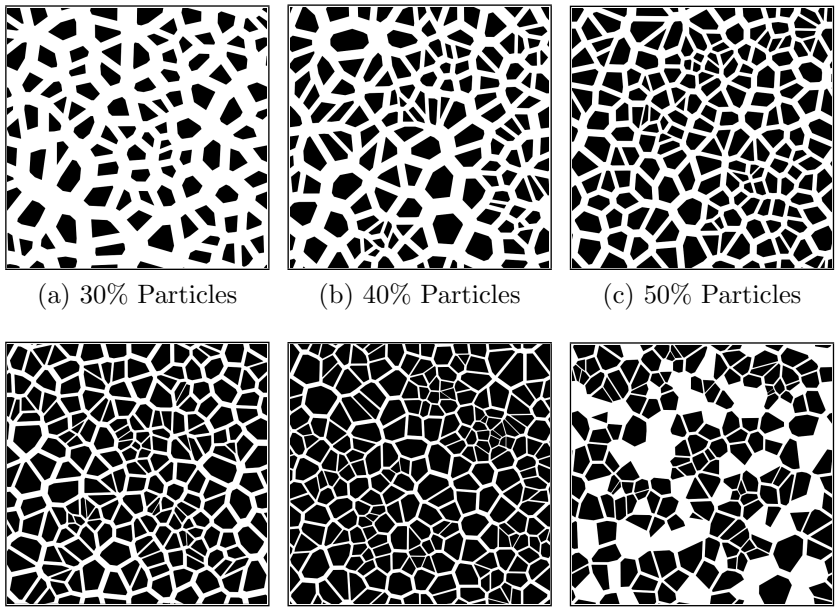

(a) 30% Particles (b) 40% Particles (c) 50% Particles

(d) 60% Particles (e) 70% Particles (f) 50% Particles with MA

Figure 2: Two-phase microstructures with varying percentage particulates

of the simulation. For initial tests it was assumed that the particles were perfectly bonded to the matrix and that the crack could only grow through the matrix phase.

The microstructures were subjected to a fixed strain rate of 1×10^{-4} s^{-1} in both the positive and negative X direction as shown in Figure 3. The Young's modulus, E, and Poisson's ratio, ν, are as shown in Table 1. It should be noted that the elastic constants of each phase are not representative of any particular material, but they can be selected to represent real phases within a microstructure.

The arbitrary crack propagation model implemented allows prediction of crack propagation along internal control volume faces [19]. An internal con-

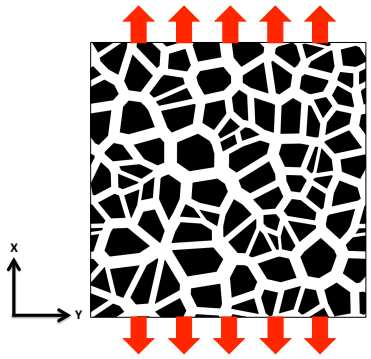

Figure 3: Generated microstructure with applied traction

Table 1: Material properties

	E [GPa]	ν
Primary Phase	900	0.1
Secondary Phase	150	0.25

trol volume face at which the failure criterion is satisfied is turned into a pair of cohesive zone boundary faces. The traction force specified between these cohesive zone faces is governed by the cohesive zone model. The cohesive zone model works on the basis that all the damage processes taking place locally ahead of the crack tip can be described by a unique traction-displacement relationship as shown in Figure 4. For all the simulations in the current work a Dugdale cohesive zone model was employed.

Once the critical traction, σ_{max}, reaches the normal cohesive traction, the value of σ decreases from the critical traction to zero according to the specified traction-separation curve. When the critical normal separation, δ_c, is reached, fracture is assumed to have taken place and the cohesive faces are thereafter treated as traction-free faces.

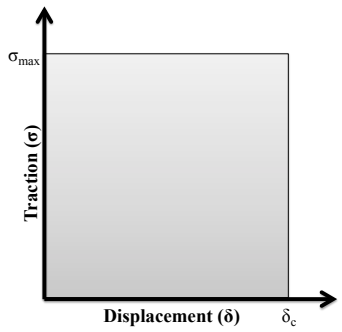

Figure 4: Dugdale cohesive traction-displacement law

A complete description of the algorithm including details of the special treatment of discretisation of traction at a material interface can be found in Carolan et al. [9] and Tukovic et al. [37].

4. Results and Discussion

4.1. Strength analysis

4.1.1. Effect of percentage particulates

As the particle content increases the overall stiffness of the bulk material increases, as can be shown by the Hashin-Shtrikman bounds [42–44]. Similarly, it was found that the microstructures showed an increase in strength with an increase in the percentage particulates, see Figure 5. Several authors [45–48] have shown experimentally that the strength of some two-phase ceramic composites increases as the volume fraction of the interpenetrating second phase decreases. However, it was noted that there was a levelling off in strength between 30% and 40% particulates. This may indicate that the interaction between the particles becomes negligible at lower volume fractions and failure is purely due to interactions between the grain and matrix.

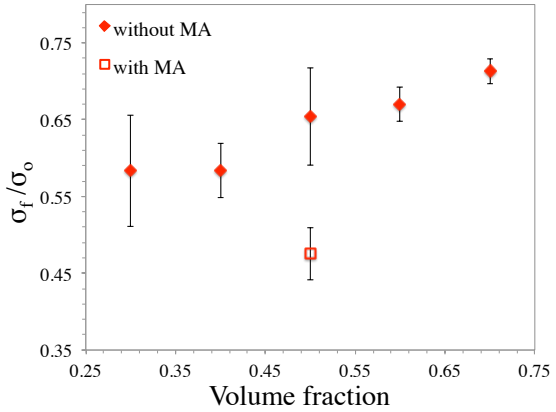

Figure 5: Effect of varying the percentage particulates. Flexural strength is normalised with respect to the cohesive strength

Figures 6a to 6f compare the stress distributions in the XX, YY and ZZ directions for a microstructure with 30% and 70% grains. It is apparent that the microstructure with 30% grains is more highly stressed in each direction. The larger volume fraction of grains in the 70% microstructure constrains the matrix more resulting in a reduction in the high stress gradients. The matrix is the weakest link in the microstructures, hence reducing the high stresses increases the strength.

It was also noted that the strength of the microstructures with the matrix agglomerations were consistently lower than the equivalent 50% microstructures without the matrix agglomerations. This is in agreement with Spowart [49] who has shown that there is a direct relationship between the strength of reinforced alumina composites and the homogeneity of the reinforcement particles. The authors have previously shown [36] that the matrix agglomerations result in an increase in localised stress concentrations. Similarly,

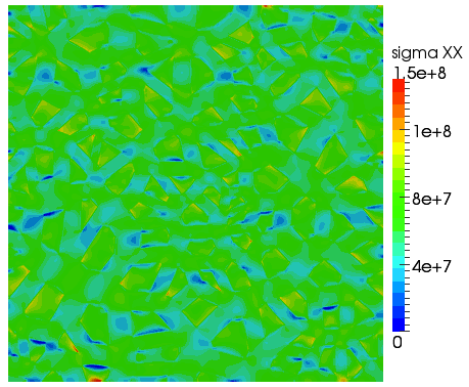

(a) σ_{xx} for 30% Particles

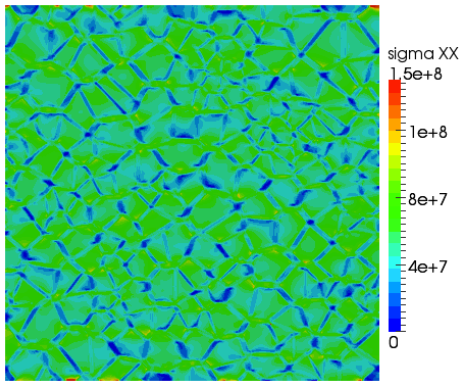

(b) σ_{xx} for 70% Particles

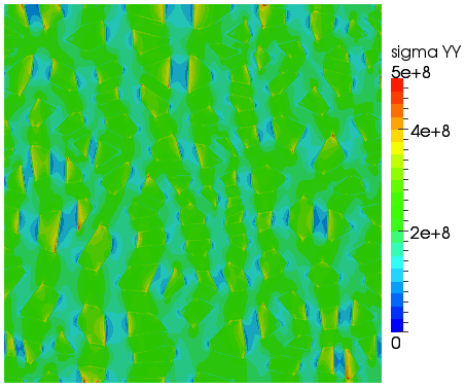

(c) σ_{yy} for 30% Particles

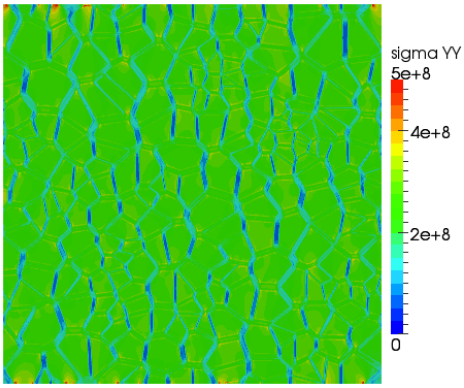

(d) σ_{yy} for 70% Particles

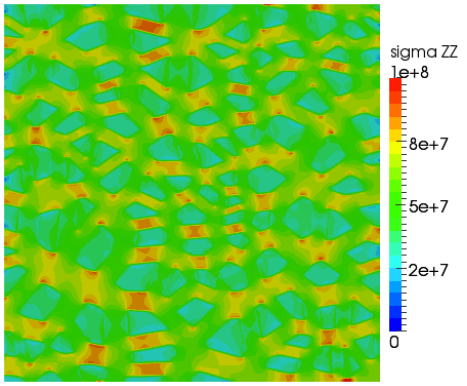

(e) σ_{zz} for 30% Particles

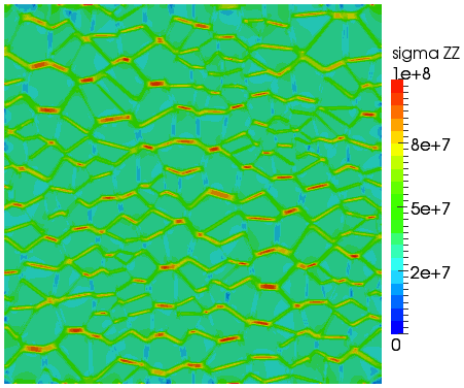

(f) σ_{zz} for 70% Particles

Figure 6: Comparison of stress distributions for microstructure with 30% particles and 70% particles, showing higher local stresses in microstructure with 30% particles.

Chawla et al. [3, 50] found that the inclusion of regions filled predominantly with the second phase material caused an increase in stress concentrations in nearby clusters of particles. This is clearly visible from Figure 7. Furthermore, it can be observed from Figure 8 that the crack initiates between two particles which have matrix agglomerations on either side.

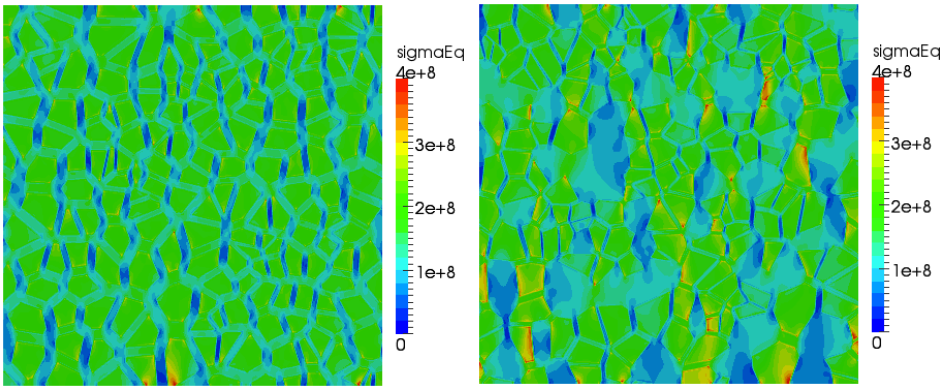

(a) Stress in 50% microstructure

(b) Stress in 50% microstructure with MA

Figure 7: Comparison of average stresses in 50% microstructures with and without matrix agglomerations

4.1.2. Effect of Young's modulus

The Young's modulus value of the matrix material, E_2, was varied from 150 GPa up to 400 GPa to investigate the effect of matrix stiffness on the strength of the overall bulk material. It should be noted that the Poisson's ratio of the matrix was kept constant. It was found that the strength of the bulk material increased as the Young's modulus of the second phase increased, see Figure 9. As the Young's modulus of the second phase material increases, the elastic mismatch between the matrix and the particulates decreases. This results in an overall decrease in stress concentrations through-

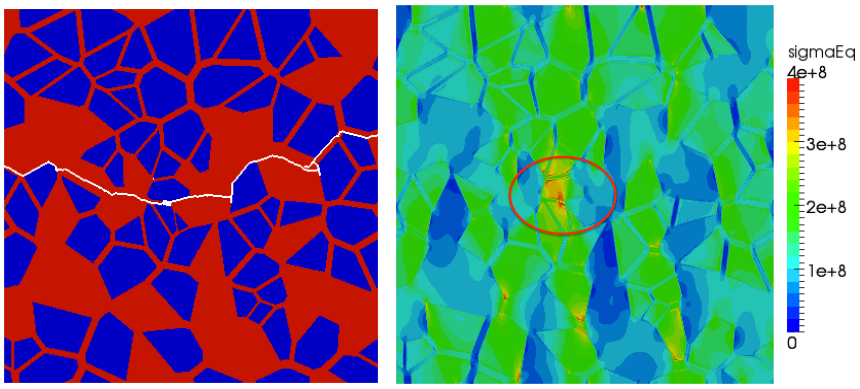

(a) Crack path (b) Stress in microstructure

Figure 8: Crack propagation and the Von Mises equivalent stresses with the crack initiation circled in red for a microstructure with matrix agglomerations

out the microstructure. From Figure 9 it may also be observed that as the material becomes more homogenous, there is a decrease in the amount of scatter in the results.

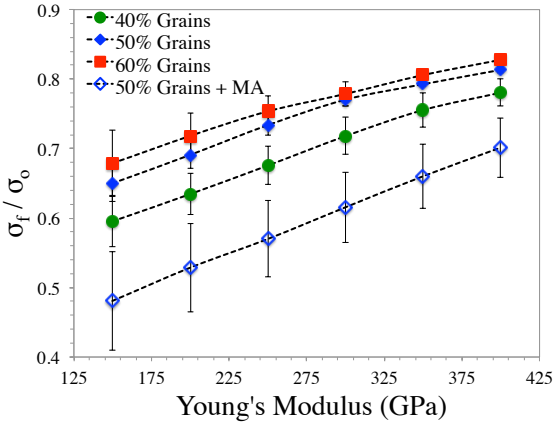

Figure 9: Effect of varying the Young's modulus of the matrix material. Flexural strength is normalised with respect to the cohesive strength

The effect of increasing the elastic modulus of the second phase material decreased as the percentage particulates increased. The microstructures with

40%, 50% and 60% particulates where found to increase in strength by 31.1%, 25.2% and 22.0% respectively. From Table 2 it can be seen that the increase in E_2 for the microstructure with 40% particulates results in the largest increase in the overall Young's modulus value.

Table 2: Young's modulus values for the bulk material for E_2 equal to 150 GPa and 400 GPa using the Mori-Tanaka method [51]

	E_2 = 150 GPa	E_2 = 400 GPa	ΔE
40% Particles	250 GPa	534 GPa	113.6%
50% Particles	291 GPa	578 GPa	98.6%
60% Particles	343 GPa	626 GPa	82.5%

4.2. Isotropy

The isotropic properties of the microstructures were investigated. In addition to the above mentioned analysis, each microstructure was subjected to a fixed strain rate of 1×10^{-4} s^{-1} in the positive and negative Y direction. The stress and strain in each microstructure was measured and the Young's modulus value was calculated using the homogenisation approach outlined in [52]. From Figure 10 it can be observed that the elastic properties of the microstructures are isotropic. It should also be noted that the Young's modulus value for the microstructure with the matrix agglomerations was in agreement with the 50% microstructure with no matrix agglomerations, showing that the elastic properties are only affected by the volume fraction of each phase and not by their distribution. This has previously been shown in [36].

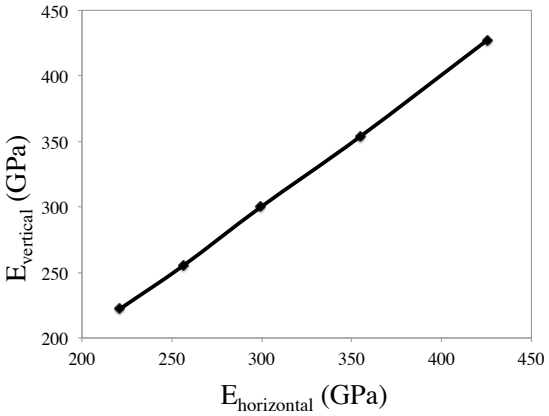

Figure 10: Isotropic Young's modulus of microstructures

The isotropic strength properties were also investigated. Figure 11 shows that there is little difference between the microstructure loaded in the X and Y direction, showing the microstructures are also isotropic in terms of strength.

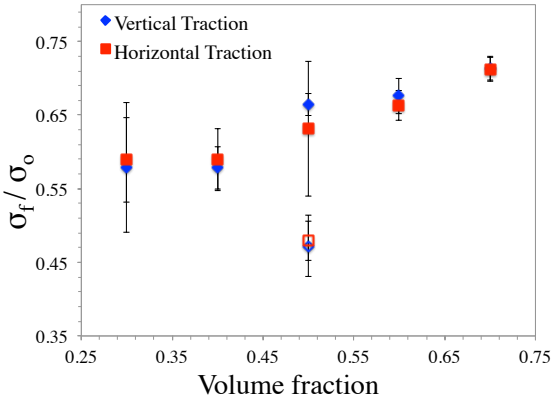

Figure 11: Isotropic strength of microstructures with varying volume fractions of particulates

4.3. Matrix agglomerations

To further investigate the effect of matrix agglomerations on the elastic and strength properties, additional microstructures with varying amounts and shapes of matrix agglomerations were generated. In all cases the volume fraction of each phase was kept close to 50%. In order to investigate the effect of the amount of matrix agglomerations, the number of grains removed to create matrix agglomerations was varied from 10% to 70% of the total number of grains, while ensuring the overall particle content remained constant. Figure 12 shows the microstructures with varying amount of matrix agglomerations.

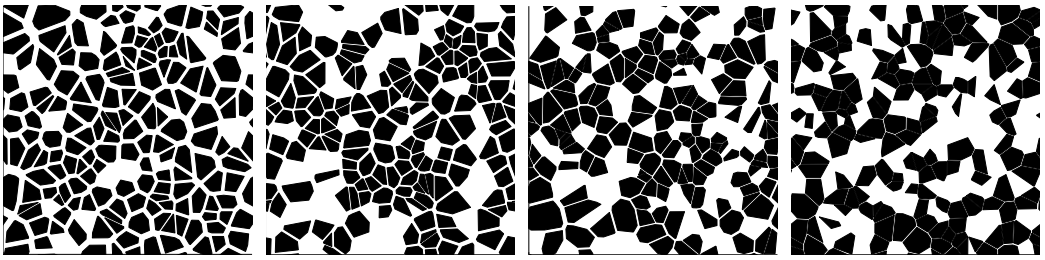

(a) 10% MA (b) 30% MA (c) 50% MA (d) 70% MA

Figure 12: Microstructures with 50% particles and varying amount of matrix agglomerations.

The effect of matrix agglomeration shape was investigated by removing 15 grains from each microstructure in various shapes as shown in Figure 13. By removing a fixed number of grains, it was ensured that the percentage matrix agglomerations in each microstructure remained constant. In addition the microstructures in Figures 13c and 13d were rotated 90°.

In each case the elastic properties of the microstructures were calculated using the homogenisation approach. Figure 14 shows the elastic properties

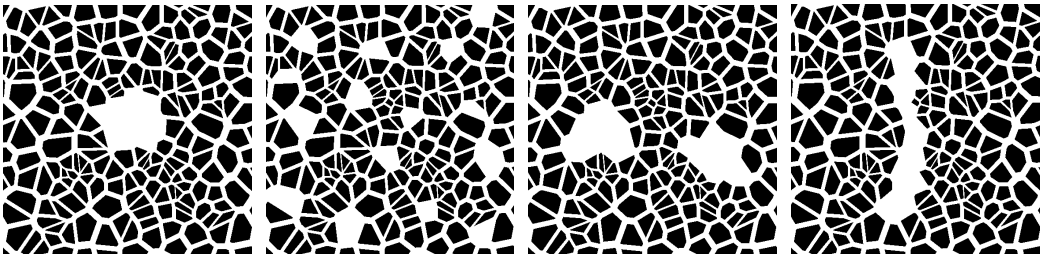

(a) Shape 1 (b) Shape 2 (c) Shape 3 (d) Shape 4

Figure 13: Microstructures with 50% particles and matrix agglomerations with various shapes.

for the microstructures both with and without matrix agglomerations plotted along side the calculated Mori-Tanaka values. In all cases it was found that the elastic properties were in agreement with the Mori-Tanaka values, once again showing that matrix agglomerations do not affect the elastic properties of the microstructures.

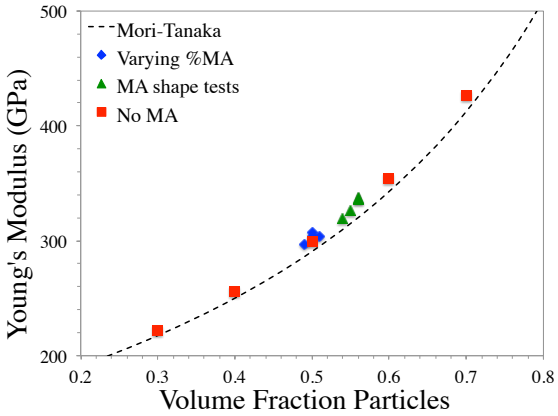

Figure 14: Graph showing the variation in Young's modulus with volume fraction of grains for microstructures with varying amount and shape of matrix agglomerations. The elastic properties of the microstructures without matrix agglomerations are also shown for comparison.

In addition, the effect of the matrix agglomerations on the isotropic

strength properties was also investigated as outlined in Section 4.1. Figure 15 shows the results for the microstructures with varying amounts of matrix agglomerations.

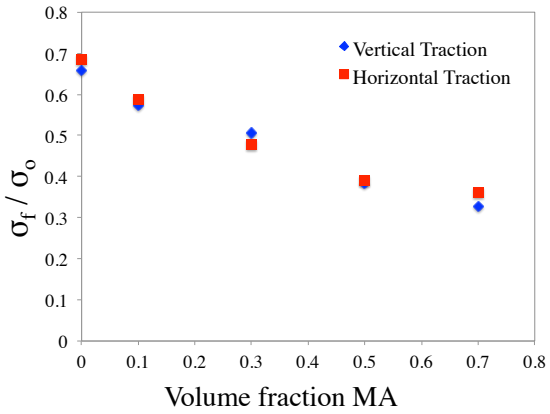

Figure 15: Graph showing the isotropic strength data for microstructures with varying amounts of matrix agglomerations.

From Figure 15, it is clearly evident that the strength of the microstructures is strongly affected by the amount of matrix agglomerations. However, similar to Figure 11, it can be seen that there is little variation between the microstructures loaded vertically and horizontally. This shows that the microstructures with varying amounts of matrix agglomerations are still isotropic in terms of their strength properties.

Furthermore, the microstructures with varying matrix agglomeration shapes were found to vary by only 0.9%, 1%, 2.3% and 0.4% when loaded vertically and horizontally. Hence it has been demonstrated that the microstructures are isotropic in terms of both strength and elastic properties.

5. Conclusion

In this paper a modified Voronoi tessellation approach has been implemented to generate two-dimensional micromechanical models of two-phased ceramic composites. Finite volume analysis was carried out on these synthetic microstructures to investigate their mechanical properties, such as strength and Young's modulus. Based on the simulation results and the observations made, the following conclusions can be drawn.

1. The strength of the ceramic composites increases as the volume fraction of hard particles increases.
2. The strength of the microstructures are strongly affected by the distribution of the primary phase.
3. Increasing the Young's modulus value of the second phase results in an increase in the overall strength of the microstructure.
4. The microstructures are found to be isotropic in terms of both strength and elastic parameters.
5. The elastic properties of the microstructures are not affected by the homogeneity of the microstructure.

6. Acknowledgements

The authors would like to thank Element Six Ltd., Enterprise Ireland and the Irish Research Council for providing financial support for this research.

7. References

[1] M.W. Cook, P.K. Bossom. Trends and recent developments in the material manufacture and cutting tool application of polycrystalline dia-

mond and polycrystalline cubic boron nitride. Int. J. Refract. Met. Hard Mater., 18 (2000) 147 –152

[2] M. Groeber, S. Ghosh, M.D. Uchic, D.M. Dimiduk. A framework for automated analysis and simulation of 3D polycrystalline microstructures. Part 2: Synthetic structure generation. Acta Mater. 56:6 (2008) 1274–1287

[3] A. Ayyar, N. Chawla. Microstructure-based modeling of crack growth in particle reinforced composites. Composite Science and Technology. 66:13 (2006) 1980–1994

[4] P. Chantikul, S.J. Bennison, B.R. Lawn. Role of Grain Size in the Strength and R-Curve Properties of Alumina. J. Am. Ceram. Soc. 73:8 (1990) 2419–2427

[5] J.P. Singh, A.V. Virkar, D.K. Shetty, R.S. Gordon. Strength-Grain Size Relations in Polycrystalline Ceramics. J. Am. Ceram. Soc. 62:3-4 (1978) 179–183

[6] R.F. Cook, B.R. Lawn, C.J. Fairbanks. Microstructure-Strength Properties in Ceramics; I, Effect of Crack Size on Toughness. J. Am. Ceram. Soc. 68:11 (1985) 604–615

[7] D. Carolan, P. Alveen, A. Ivanković, N. Murphy. Effect of notch root radius on fracture toughness of polycrystalline cubic boron nitride. Eng. Fract. Mech., 78 (2011) 2885–2895

[8] D. Carolan, A. Ivanković, N. Murphy. Thermal shock resistance of polycrystalline cubic boron nitride. J. Eur. Ceram. Soc., 32 (2012) 2581–2586

[9] D. Carolan, Ž. Tuković, N. Murphy, A. Ivanković. Arbitrary crack propagation in multi-phase materials using the finite volume method. Comp. Mater. Sci., 69 (2013) 153–159

[10] I. Demirdžić, D. Martinović, A. Ivanković. Numerical simulation of thermal deformation in welded workpiece. Zavarivanje 31 (1988) 209–219.

[11] I. Demirdžić, D. Martinović. Finite volume method for thermo-elasto-plastic stress analysis. Comput. Method. Appl. M., 109:3-4 (1993) 331–349.

[12] I. Demirdžić, S. Muzaferija. Finite volume method for stress analysis in complex domains. Int. J. Numer. Meth. Engng., 37 (1994) 3751–3766.

[13] I. Demirdžić, S. Muzaferija. Numerical method for coupled fluid flow, heat transfer and stress analysis using unstructured moving meshes with cells of arbitrary topology. Comput. Method. Appl. M., 125 (1995) 235–255.

[14] I. Demirdžić, E. Džaferović, A. Ivanković. Finite-volume approach to thermoviscoelasticity. Numer. Heat Tr. B-Fund, 47 (3) (2005) 213–237.

[15] A. Ivanković, I. Demirdžić, J. Williams, P. Leevers. Application of the finite volume method to the analysis of dynamic fracture problems. Int. J. Fract., 66:4 (1994) 357–371.

[16] A. Ivanković, S. Muzaferija, I. Demirdžić. Finite volume method and multigrid acceleration in modelling of rapid crack propagation in full-scale pipe test. Comput. Mech., 20 (1997) 46-52.

[17] A. Ivanković. Finite Volume Modeling of Dynamic Fracture Problems. Computer Modelling and Simulation in Engineering, 4 (1999) 227–235.

[18] A. Ivanković, K. Pandya, J. Williams. Crack growth predictions in polyethylene using measured tractionseparation curves. Eng. Fract. Mech., 71:4-6 (2004) 657668.

[19] N. Murphy, A. Ivankovic. The prediction o dynamic fracture evolution in PMMA using a cohesive zone model. Eng. Fract. Mech., 72:6 (2005) 861–875

[20] V. Kanyanta, A. Ivanković, A. Karac. Validation of a fluidstructure interaction numerical model for predicting flow transients in arteries. J. Biomech., 42:11 (2009) 1705–1712.

[21] A. Karac, A. Ivanković. Investigating the behaviour of fluid-filled polyethylene containers under base drop impact: A combined experimental/numerical approach. Int. J. Impact Eng., 36:4 (2009) 621631.

[22] L. Madej, L. Rauch, K. Perzynski, P. Cybulka. Digital Material Representation as an efficient tool for strain inhomogeneities analysis at the micro scale level. Archives of Civil and mechanical Engineering, XI(3) (2011) 661–679

[23] P. Zhang, M. Karimpour, D. Balint, J. Lin, D. Farrugia. A controlled Poisson Voronoi tessellation for grain and cohesive boundary generation applied to crystal plasticity analysis. Comp. Mater. Sci., March (2012) 2–7

[24] R. Dobosz, M. Lewandowska, K.J. Kurzydlowski. FEM modelling of the combined effect of grain boundaries and second phase particles on the flow stress of nanocrystalline metals. Comp. Mater. Sci., 53:1 (2012) 286–293

[25] M. Nygårds, P. Gudmundson. Three-dimensional periodic Voronoi grain models and micromechanical FE-simulations of a two- phase steel. Comp. Mater. Sci., 24 (2002) 513–519

[26] M. Kühn, M.O. Steinhauser. Modeling and simulation of microstructures using power diagrams: Proof of the concept. Appl. Phys. Lett., 93 (2008) 034102

[27] H.D. Espinosa, P.D. Zavattieri. A grain level model for the study of failure initiation and evolution in polycrystalline brittle materials. Part I: Theory and numerical implementation. Mech. Mater., 35 (2003) 333–364

[28] D.H. Warner, J.F. Molinari. Micromechanical finite element modeling of compressive fracture in confined alumina ceramic. Acta Mater., 54:19 (2006) 5135–5145

[29] T. Zhou, C. Huang, H. Liu, J. Wang, B. Zou, H Zhu. Crack propagation simulation in microstructure of ceramic tool materials. Comp. Mater. Sci., 54 (2012) 150–156

[30] D. Wang, J. Zhao, Y. Zhou, X. Chen, A. Li, Z. Gong. Extended finite element modeling of crack propagation in ceramic tool materials by

considering the microstructural features. Comp. Mater. Sci., 77 (2013) 236–244

[31] M. Danielsson, D.M. Parks, M.C. Boyce. Micromechanics, macromechanics and constitutive modeling of the elasto-viscoplastic deformation of rubber-toughened glassy polymers. J. Mech. Phys. Solids, 55:3 (2007) 533–561

[32] P Zhang, D Balint, J Lin. An integrated scheme for crystal plasticity analysis: Virtual grain structure generation. Comp. Mater. Sci., 50 (2011) 2854–2864

[33] P. Zhang, D. Balint, J. Lin, Controlled Poisson Voronoi tessellation for virtual grain structure generation: a statistical evaluation. Philos. Mag. 91:36 (2011) 4555–4573

[34] H. Li, K. Li, G. Subhash, L.J. Kecskes, R.J. Dowding. Micromechanical modeling of tungsten-based bulk metallic glass matrix composites. Mater. Sci. Eng. A, 429 (2006) 115–123

[35] Y. Wang, L. Shuhua, P. Xiao, J. Zou. FEM simulations of tensile deformation and fracture analysis for CuW alloys at mesoscopic level. Comp. Mater. Sci., 50 (2011) 3450–3454

[36] P. Alveen, D. Carolan, D. NcNamara, N. Murphy, A. Ivanković. Micromechanical modelling of ceramic based composites with statistically representative synthetic microstructures. Comp. Mater. Sci., 79 (2013) 960–970

[37] Ž. Tuković, A. Ivankovic, A. Karač. Finite-volume stress analysis in multi-material linear elastic body. Int. J. Numer. Meth. Engng., 93:4 (2013) 400-419

[38] H. Weller, G. Tabor, H. Jasak, C. Fureby. A tensorial approach to CFD using object oriented techniques. Computers in Physics, 12 (1998) 620–631

[39] The OpenFOAM Foundation, www.openfoam.com, 2014

[40] The OpenFOAM Extend Project, www.extend-project.de, 2014

[41] P. Zhang, M. Karimpour, D. Balint, J. Lin, D. Farrugia. A controlled Poisson Voronoi tessellation for grain and cohesive boundary generation applied to crystal plasticity. Comp. Mater. Sci., 64 (2012) 84–89

[42] Z. Hashin, S. Shtrikman. A variational approach to the theory of the elastic behaviour of multiphase materials. J. Mech. Phys. Solids, 11 (1963) 127–140

[43] P. Wall. A comparison of homogenization, Hashin-Shtrikman bounds and the Halpin-Tsai equation. Applications of Mathematics, 42 (1997) 245–257

[44] Z. Hashin. On elastic behaviour of fibre reinforced materials of arbitrary transverse phase geometry. J. Mech. Phys. Solids, 13 (1965)119–134

[45] Y.F. Yang, Q.C. Jiang. Reaction behaviour, microstructure and mechanical properties of TiC-TiB_2/Ni composites fabricated by pressure

assisted self-propagating high-temperature synthesis in air and vacuum. Mater. Design, 49 (2013) 123–129

[46] S. Schicker, T. Erny, D.E. García, R. Janssen, N. Claussen. Microstructure and mechanical properties of Al-assisted sintered Fe/Al_2O_3 cermets. J. Eur. Ceram. Soc., 19 (1999) 2455–2463

[47] S.C. Zhang, G.E. Hilmas, W.G. Fahrenholtz. Mechanical properties of sintered ZrB_2-SiC ceramics. J. Eur. Ceram. Soc., 31 (2011) 893–901

[48] J. Lui, P.D. Ownby. Boron carbide reinforced alumina composites. J. Am. Ceram. Soc., 74:3 (1991) 674–677

[49] J.E. Spowart. Microstructural characterization and modeling of discontinuously-reinforced aluminum composites. Mater. Sci. Eng. A, 425 (2006) 225–237

[50] N. Chawla, B.V. Patel, M. Koopman, K.K. Chawla, R. Saha, B.R. Patterson, E.R. Fuller, S.A. Langer. Microstructure-based simulation of thermomechanical behavior of composite materials by object-oriented finite element analysis. Mater. Charac., 49 (2003) 395–407

[51] T. Mori and K. Tanaka. Average stress in matrix and average elastic energy of materials with misfitting inclusions. Acta Metall., 21 (1973) 571– 574

[52] X. Chen, Y. Mai. Micromechanics of rubbertoughened polymers. J. Mater. Sci., 33 (1998) 3529–3539